Influence of curvature on impurity gettering by nanocavities in Si

François Schiettekatte,[a] Carl Wintgens, and Sjoerd Roorda
*Groupe de recherche en science et technologie des couches minces et Département de physique,
Université de Montréal, Montréal, Québec, Canada, H3C 3J7*

Competition for Au gettering in Si between two cavity layers of different diameter (34 and 12 nm) is examined. Au is initially contained in the large cavity layer made by He implantation. Transport of Au towards the second, small diameter cavity layer is measured by ion scattering. The true surface in both layers is determined by electron microscopy. Small cavities are found to be four times more efficient gettering sites than large cavities for the same amount of internal surface. This difference is explained by a simple model based on curvature thermodynamics, faceting, and surface reconstruction. © *1999 American Institute of Physics.* [S0003-6951(99)03813-9]

Metallic impurities are notorious for their detrimental effect on silicon-based devices.[1] Proximity gettering to hydrogen or helium induced cavities has been found to be an efficient method to control the impurity concentration in the active area of these devices,[2,3] especially for monovalent atoms such as Cu, Ag, Pt, and Au. Recently, Myers *et al.* determined ΔG, the binding free energy, for several transition metal contaminations in silicon[4,5] trapped at such cavities. For Au, this energy was deduced from the detrapping kinetics and found to be near 2.4 eV. Nanocavities act as gettering sites, probably because they contain a pure, unoxidized, and almost uncontaminated surface, but that in itself does not explain the large value of ΔG found by Myers *et al.* The binding energy was also found to decrease with increasing cavity formation temperature. The authors suggested that this effect resulted from the entropy term in the binding free energy or from changes in the chemisorption states with temperature.

We propose that the strong curvature of the nanocavities contributes to its gettering efficiency. The curvature of a surface changes the surface energy due to capillary and surface tension effects.[6] Especially, it influences the chemical potential μ of adsorbed atoms proportionally to the surface curvature. Given $[i]$ a fraction of interstitial impurities present in a bulk material in equilibrium with cavity surfaces for which θ is the average fraction of occupied sites. In the case of a weakly contaminated cavity ($\theta \ll 1$), the chemical potential of this system can be expressed as

$$\mu_0 + kT \ln[i] = kT \ln\left[\frac{\theta}{1-\theta}\right] - \beta, \quad \beta = \frac{2\gamma}{R}\frac{V^{\text{mol}}}{N_A}. \quad (1)$$

The first term on right hand side is the Langmuir isotherm[6] for a flat surface. β is the curvature contribution to the chemical potential for which γ is the surface tension of a cavity while R is its radius. V^{mol} is the molar volume of the bulk material and N_A the Avogadro's number. Thus, it appears that a layer formed on a curved surface will be energetically favorable. Moreover, the $1/R$ dependency should make smaller cavities more efficient than larger ones.

In order to verify if this assumption holds for metallic impurities adsorbed on a cavity surface, we measured the impurity transport and equilibrium between two layers with cavities of different diameters. Cavities are usually formed by implanting He or H followed by annealing. Their size, and consequently the curvature of their surface, is mainly determined by the annealing temperature after H or He implantation, as shown by early experiments.[7]

Samples used in this study were $\langle 100 \rangle$ Czochralski (Cz) silicon wafers (*n*-type, 10–15 Ω cm, 500 μm thick). He ions were first implanted into the samples with a dose of 1×10^{17} cm^{-2} at an energy of 100 keV at room temperature. Wafers were then annealed in vacuum at 1273 K for 1 h in order to form a layer of large nanometer-size cavities. The samples were further implanted with Au ions to a dose of 1×10^{14} cm^{-2}, followed by annealing at 1173 K for 3 h to induce gettering of the implanted impurities to the first cavity layer. A second layer of smaller cavities was obtained by implanting 30 keV He ions to a dose of 3×10^{16} cm^{-2}. Finally, a series of isothermal anneals was performed at 1073 K in order to form the second layer of nanocavities and to observe the redistribution of Au between layers.

The density and size of nanocavities in each layer were determined by cross-sectional transmission electron microscopy (XTEM) carried out in bright field mode on a Philips CM-30 microscope operating at 300 kV. A micrograph with both cavity layers is shown in Fig. 1. As reported under *interlayer data* in Table I, the cavities in the first layer, formed at 1273 K, have a mean diameter $\varnothing_1$ of 31 nm. The distribution follows the implanted He depth profile, which has a mean range of 700 nm. The mean diameter $\varnothing_2$ of the cavities in the second layer is 12 nm. This layer was formed during the 1073 K annealing. It is known that within 15 min at 1073 K, the cavity size stabilizes at this value.[7] The ratio of true surface amount in layer 2 over layer 1 (A_2/A_1) is also calculated. However, a more careful examination of Fig. 1 reveals that the back end of layer 1 is populated with a significant amount of small cavities. Their size is comparable to those in layer 2 and their number is about 1/3 of the total number of cavities in layer 2. The remaining large cavities in layer 1 have an average diameter of 34 nm. The ratio A_2/A_1, which now designates the surface ratio of small to large cavi-

---

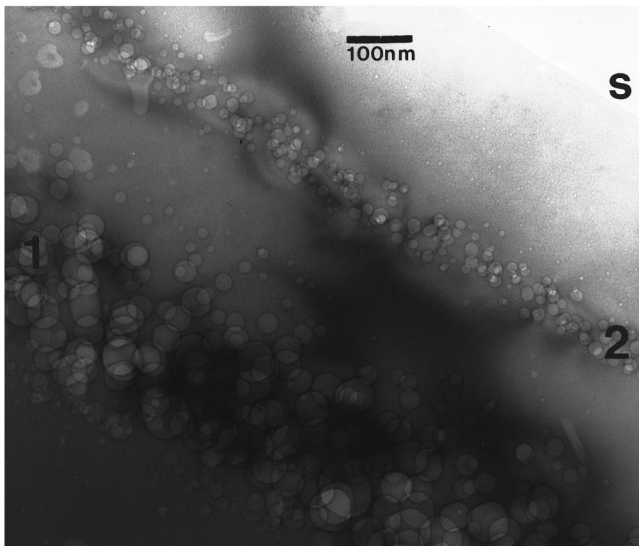[a]Electronic mail: francois.schiettekatte@umontreal.ca

FIG. 1. XTEM micrograph of a sample with two cavity layers. (1) first layer, (2) second layer, (s) surface.

ties, is also increased as shown in Table I under *small vs large cavities*.

In order to establish the relative gettering efficiency of the two cavity layers, the impurity transport process between them was examined. Depth profiles of redistributed Au were measured by Rutherford backscattering spectrometry (RBS) employing 2 MeV He ions scattered through 170°. The sample holder was tilted 5° off the incident beam to avoid channelling. The time progression of the Au concentration in both cavity layers during the second annealing is illustrated in Fig. 2. A Au peak progressively appears in the region of layer 2. After 1 h of annealing only a relatively small amount of Au reached the layer 2. Also, it appears that Au in layer 1 decreases asymmetrically. In fact, the Au concentration in the back end of layer 1 remains almost constant. Because the Au profiles were both measured at equilibrium (before and after introduction of the second cavity layer) it follows immediately that the binding energy is larger in the smaller cavities (backside of the peak) than in the larger cavities (front side of the peak).

TABLE I. Diameters ($\varnothing$) and area ratio extracted from Fig. 1; ratio of Au concentration Q_i in each layer at equilibrium from Fig. 3 and relative efficiency of layer 2 over layer 1 per unit area of cavity surface; fitting parameters of Eq. (2) to Fig. 3; resulting $\beta_2 - \beta_1$.

	Interlayer data	Small vs large cavities
$\varnothing_1$ [nm]	31 ± 15[a]	34 ± 13[a]
$\varnothing_2$ [nm]	12 ± 5[a]	12 ± 5[a]
A_2/A_1	0.13 ± 0.01	0.16
Q_2/Q_1 at $t \to \infty$	0.40 ± 0.01	0.65
Efficiency	3.1	4.1
Q_T [Au/nm^2]	1.06	1.06
α	0.72 ± 0.01	0.6
τ [h]	1.8 ± 0.1	$\cdots$
$\beta_2 - \beta_1$ calculated		43 ± 16 meV
$\beta_2 - \beta_1$ for $S_2/S_1 \approx A_2/A_1$		130 meV
k_1/k_2 for calculated $\beta_2 - \beta_1$		$40 \pm 7\%$

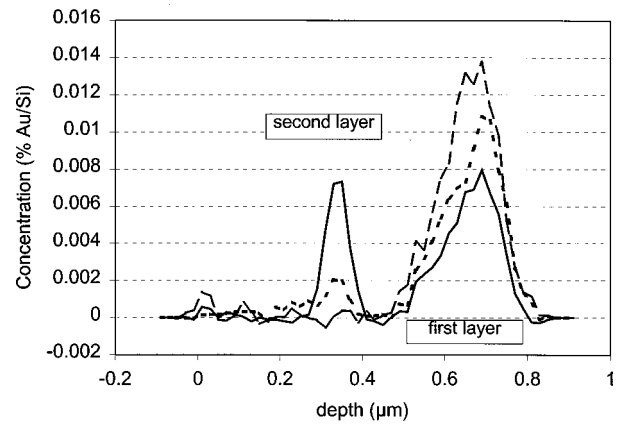[a]Standard deviation over cavity population.

FIG. 2. Au depth profile evolution with time during annealing of second cavity layer at 1073 K; after 0 (– – –), 1 (----), and 30 h (—)

The Au concentration in each layer and at the surface is plotted in Fig. 3 against the duration of the second annealing. While the surface Au concentration is constant and negligible, the total concentration decreases with time. This is due to the fact that the Au interstitials are progressively lost to the bulk until their concentration throughout the sample depth is in equilibrium with the gettering sites. From Fig. 3, the amount of ''lost'' Au at equilibrium is 2.1×10^{13} Au/cm^2. Divided by the sample thickness (0.05 cm), this gives 4.2×10^{14} Au/cm^3, which corresponds to the substitutional Au solubility at 1073 K.[1] It is also seen in Fig. 3 that it takes several hours before appreciable Au is trapped at the small cavity layer. Because this is more than the 15 min. required for cavity formation, these two processes can be treated as independent.

After long-term equilibrium has been reached, the ratio of Au trapped in both cavity layers is $Q_2/Q_1 = 0.40$ whereas the ratio of surface area is only $A_2/A_1 = 0.13$. We thus find that for an equivalent amount of cavity surface, the cavities in layer 2 are three times more efficient than those of layer 1. Knowing that the smaller cavities are more efficient gettering sites than the larger cavities, we now attribute the asymmetry in the RBS signal to the uneven size distribution of cavities in layer 1. Apparently, only the Au from the large cavities situated between 500 and 700 nm (about 5/6 of the Au) is
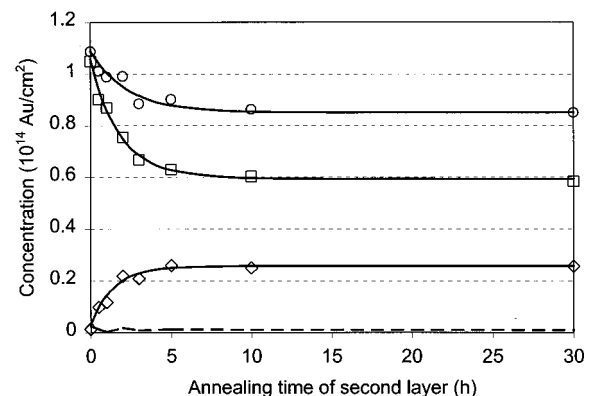

FIG. 3. Evolution of Au concentration in layer 1 ($\square$), layer 2 ($\diamond$) and at surface (– – –) during second annealing (at 1073 K). Total concentration also appears ($\bigcirc$).

redistributed, and this has been taken into account in the second column of Table I, labeled ''*small vs large cavities*.'' This result demonstrates that small 12 nm cavities are in fact 4.1 times more efficient than large 34 nm cavities for the same amount of cavity surface.

Concerning the transient part of Fig. 3, the present experiment can be treated as two thin cavity layers separated by the distance Δx and exchanging interstitial impurities in a steady-state diffusion process.[5] All the Q_T impurities are contained in layer 1 at time $t=0$. Through Eq. (1), and for small contamination ($\theta \ll 1$), it can be shown that the Au concentration Q_n in each layer is expressed by

$$Q_1(t,T)=Q_T-Q_2(t,T)=Q_T[(1-\alpha)e^{-t/\tau}+\alpha], \qquad (2)$$

where α is the fraction of impurities remaining in layer 1 at equilibrium ($t \gg \tau$) and

$$\tau=\left[\frac{\alpha S_2}{e^{-(\mu_0+\beta_2)/kT}}\frac{\Delta x}{N_{Si}D_{imp}}\right]. \qquad (3)$$

Here, N_{Si} is the atom density of silicon and D_{imp} the diffusion coefficient of the impurities in their interstitial state. S_2 is the areal density of sites in layer 2 ($\theta_n=Q_n/S_n$). Consequently, $\mu_0+\beta_2$, the effective chemical potential for cavity layer 2, can be deduced from τ, provided that the other parameters of Eq. (3) are known.

A least-squares fit of Eq. (2) was applied to the Au concentration evolution in both cavity layers and appears as solid lines in Fig. 3. These equations were weighted by a function of the form $(1-\lambda_1)\exp(-\lambda_2 t)+\lambda_1$ to take into account the lost Au dissolved into the bulk. The parameters returned by this fit are shown in Table I. With an interstitial Au diffusivity[1] of $D_{imp}=3.5\times10^{-6}$ cm²/s, assuming $S_2=1.5\times10^{14}$ cm⁻², and with $\Delta x=400$ nm, we find from Eq. (3) that $\mu_0+\beta_2=2.5\pm0.1$ eV. This is close to the above-mentioned value of ΔG in Ref. 5. The uncertainty in $\mu_0+\beta_2$ is mainly due to the uncertainty in S_2 and D_{imp}.

Let us now evaluate if the difference in gettering efficiency is indeed a consequence of capillary effects. First, a value for β can be predicted [Eq. (1)]. Given $a=0.543$ nm the Si lattice parameter, $V^{mol}/N_A=a^3/8$. For a solid surface where an areal density n of bonds of energy ϕ are broken, $\gamma=fn\phi/2$ where f is a geometrical factor between 1 and $\sqrt{3}$ for vicinal surfaces.[6] The density of dangling bonds $n=4/a^2\sqrt{3}$ for a unreconstructed $\langle 111 \rangle$ surface and $\sqrt{3}$ larger for an unreconstructed $\langle 100 \rangle$ surface. From these definitions we find,

$$\beta=\phi\frac{f}{2\sqrt{3}}\frac{a}{R}. \qquad (4)$$

The cavities of layer 1 appear faceted in the $\langle 111 \rangle$ direction, therefore we assume $f_1\approx1$. With $\phi=1.8$ eV for Si–Si bonds, we find $\beta_1=17$ meV. For layer 2, the mean value of f_2 falls between 1 and $\sqrt{3}$ depending on the orientation. Consequently, β_2 ranges from 44 to 76 meV. The effect of curvature on the binding energy would amount to $\beta_2-\beta_1=27-59$ meV.

Based on the measured Au distribution at equilibrium (Q_1/Q_2) and for small Au coverage ($\theta \ll 1$), we can determine $\beta_2-\beta_1$ according to the difference in chemical potential [Eq. (1)]:

$$\beta_2-\beta_1=kT\ln\left[\frac{\theta_2}{\theta_1}\right]=kT\ln\left[\frac{(1-\alpha)}{\alpha}\frac{k_1A_1}{k_2A_2}\right], \qquad (5)$$

where the subscripts denote the values for each layer. While f_n already accounts for the geometrical effects on the areal density of gettering sites, k_n will do so for surface reconstruction effects, since $S_n=k_nA_n$. Assuming that the density of sites is the same within all cavities ($k_1/k_2=1$) we find from Eq. (5) that $\beta_2-\beta_1=130$ meV which is 2–4 times higher than the calculated value of $\beta_2-\beta_1$. It appears that surface reconstruction effects do play a role, and $k_1/k_2<1$.

The 7×7 and Au-induced 5×2 reconstruction of $\langle 111 \rangle$ orientation have been widely studied on the external surface of silicon.[8] For Au coverage less than 1/2 monolayer, 7×7 Au-free domains (formed above 700 K) coexist with 5×2 domains. Each 5×2 cell can accommodate seven Au atoms, instead of ten for equivalent 1×1 surface. Thus, if the large cavity surfaces were fully reconstructed, at least 35% of the bonds remain available. This is a lower limit since large cavities also contain unreconstructed curved surfaces. Moreover, it is not excluded that some reconstruction in small cavities occurs. The measured Au redistribution and the estimates of $\beta_2-\beta_1$, from curvature arguments, imply k_1/k_2 values from 33% to 47%. We thus conclude that curvature thermodynamic and surface reconstruction effects both contribute to efficient gettering in nanocavities.

In summary, experimental measurements of the Au transport between two cavity layers show that small 12 nm cavities are more efficient than large 34 nm cavities by a factor of 4.1 for equivalent amount of surface. The measured difference in *effective* trapping energy is 0.13 eV in this case. This is explained in part by the possibility of surface reconstruction in large cavities, which reduces the number of available dangling bonds, and by the effect of curvature and surface tension on the chemical potential in cavities.

[1] K. Graff, *Metal Impurities in Silicon-device Fabrication* (Springer, Berlin, 1995).

[2] S. M. Myers, D. M. Bishop, D. M. Follstaedt, H. J. Stein, and W. R. Wampler, Mater. Res. Soc. Symp. Proc. **283**, 549 (1993).

[3] J. Wong-Leung, C. E. Ascheron, M. Petravic, R. G. Elliman, and J. S. Williams, Appl. Phys. Lett. **66**, 1231 (1995).

[4] S. M. Myers, G. A. Petersen, and C. H. Seager, J. Appl. Phys. **80**, 3717 (1996).

[5] S. M. Myers and G. A. Petersen, Phys. Rev. B **57**, 7015 (1998).

[6] J. B. Hudson, *Surface Science: An Introduction* (Butterworth–Heinemann, Boston, 1991).

[7] V. Raineri, A. Battaglia, and E. Rimini, Nucl. Instrum. Methods Phys. Res. B **96**, 249 (1995).

[8] J. D. O'Mahony, J. F. McGilp, C. F. J. Flipse, P. Weightman, and F. M. Leibsle, Phys. Rev. B **49**, 2527 (1994).